



# Functional Ionic Liquid Modified Core-Shell Structured Fibrous Gel Polymer Electrolyte for Safe and Efficient Fast Charging Lithium-Ion Batteries

Xiaoxia Liu, Yufei Ren, Lan Zhang\* and Suojiang Zhang\*

Beijing Key Laboratory of Ionic Liquids Clean Process, CAS Key Laboratory of Green Process and Engineering, Institute of Process Engineering, Chinese Academy of Sciences, Beijing, China

## OPEN ACCESS

### Edited by:

Oleksandr Malyi,  
University of Oslo, Norway

### Reviewed by:

Xianhong Rui,  
Guangdong University of  
Technology, China  
Weimin Kang,  
Tianjin Polytechnic University, China  
Huarong Xia,  
Nanyang Technological  
University, Singapore

### \*Correspondence:

Lan Zhang  
zhangl@ipe.ac.cn  
Suojiang Zhang  
sjzhang@ipe.ac.cn

### Specialty section:

This article was submitted to  
Electrochemistry,  
a section of the journal  
Frontiers in Chemistry

Received: 16 March 2019

Accepted: 21 May 2019

Published: 12 June 2019

### Citation:

Liu X, Ren Y, Zhang L and Zhang S  
(2019) Functional Ionic Liquid Modified  
Core-Shell Structured Fibrous Gel  
Polymer Electrolyte for Safe and  
Efficient Fast Charging Lithium-Ion  
Batteries. *Front. Chem.* 7:421.  
doi: 10.3389/fchem.2019.00421

Fast charging is of enormous concerns in the development of power batteries, while the low conductivity and lithium ion transference number in current electrolytes degraded the charge balance, limited the rate performance, and even cause safety issues for dendrite growth. Combine inorganic fillers and ionic liquid plasticizer, here in this paper we prepared a core-shell structured nanofibrous membrane, by incorporating with carbonate based electrolyte, a gel polymer electrolyte (GPE) with high conductivity, outstanding  $\text{Li}^+$  transference number was obtained. Notably, the Li/electrolyte/ $\text{LiNi}_{0.6}\text{Co}_{0.2}\text{Mn}_{0.2}\text{O}_2$  (NCM622) half-cell with this composite electrolyte delivers a reversible capacity of 65 mAh/g at 20C, which is 13 times higher than that of with Celgard 2325 membrane. It also shows enhanced long-term cycle stability at both 3C and 5C for the suppression of lithium dendrite. This organic-inorganic co-modified GPE guarantees the fast charging ability and safety of LIBs, thus provides a promising method in high performance electrolyte design.

**Keywords:** lithium ion battery, fast charging, core-shell structure, nanofibrous separator, safety

## INTRODUCTION

With the increasing demand for energy consumption and the continuous improvement for environmental protection, the development of sustainable and renewable energy is urgently needed currently. Lithium ion batteries (LIBs) have been widely used in the power battery, energy storage applications, portable electronic equipment and other fields, owing to its inherent advantages such as high energy density, high power density, long cycle life, no memory effect, and environmental friendliness (Gao et al., 2009; Goodenough and Kim, 2010; Etacheri et al., 2011; Scrosati et al., 2011; Lu et al., 2014a; Varzi et al., 2016; Tan et al., 2018). Nevertheless, high-capacity and high-power LIBs are facing more and more challenges such as high power output, rapid charge/discharge capability and safety under dynamic conditions (Zhu et al., 2013; Xie et al., 2014; Zhang J. et al., 2014; Li et al., 2018, 2019), and it is of particularly importance to investigate methods to guarantee the safety of LIBs with enhanced fast charge capability (Rui et al., 2016; Tan et al., 2018).

LIBs generally compose of anode, cathode, electrolyte, and packing material. The electrolyte, which including polymer separator and liquid electrolyte in commercial LIBs, mainly plays two key roles: blocking the direct contact between the electrodes to avoid internal electrical short circuit and

acting as the  $\text{Li}^+$  transport passage (Tarascon and Armand, 2001; Xiao et al., 2009; Huang, 2010; Lee et al., 2014). Therefore, the electrolyte not only directly affects the LIB electrochemical performance, such as cycle stability and rate capability, but also, it has significant influence on the safety of LIBs. Most commercial LIBs adopt polyolefin [such as polyethylene (PE) and polypropylene (PP)] membranes (Huang, 2010; Kim et al., 2015; Shen et al., 2018) and  $\text{LiPF}_6$ /carbonates electrolyte, based on which satisfying cycle performances have achieved, while the rate capability and safety, especially during quick charge, is yet to be enhanced.

The major issue in fast charging LIBs is the poor kinetics caused by the sluggish ion transport in the cell, which will probably lead to large polarization and low reversible capacity, furthermore, when the anode potential is lower than that of Li plating, dendrite will be generated and may short the cell thus cause safety concerns.

Electrolyte holds significant influence on both rate capability and safety, on one hand, ionic conductivity and  $\text{Li}^+$  transference number is the major factor to control the battery kinetics (Diederichsen et al., 2017), on the other hand, the separator, which blocks the direct contact between electrodes, should also work as a physical barrier to suppress the dendrite from shorting the battery (Jana et al., 2015; Shin et al., 2015; Zheng et al., 2018). Therefore, scientist made lots of efforts in electrolyte modification, including surface coating of the separator (Ghazi et al., 2017; Liu et al., 2017a,b; Zuo et al., 2017), doping inorganic nanoparticles in polymer to obtain composite electrolyte (Xiao et al., 2012; Chen et al., 2017; Kim et al., 2017; Wang et al., 2017; Shen et al., 2018), and electrostatic spinning to get nanofibrous membrane (Choi et al., 2003; Wu et al., 2015; Ma et al., 2017; Cheng et al., 2018). Thereinto, the nanofibrous membrane has large specific surface area, three-dimensional (3D) porous structure and high electrolyte uptake ability, on which the rate capability can be enhanced (Xiao et al., 2015; Liang et al., 2016; Park et al., 2017). What's more, functional groups can be easily introduced in the electrospinning process, thereby endows the electrolyte with other properties, such as dendrite suppression (Lu et al., 2015a,b; Cheng et al., 2018; Deng et al., 2018), flame retardant (Lu et al., 2017; Jia et al., 2018; Sun et al., 2018), et al. Poly(vinylidene fluoride-co-hexafluoropropene) (PVDF-HFP) is considered as a potential polymer matrix for electrolyte not only as it has a low crystallinity which could promote rapid ion conduction (Ali et al., 2018; Zhao et al., 2019), but also, it has high dielectric constant and low surface energy that may promote the compact deposition of metal Li (Lopez et al., 2018). It is reported the ionic conductivity of PVDF-HFP-based polymer electrolytes is up to 3.9 mS/cm (Xiao et al., 2012).

Ionic liquid modified gel polymer electrolytes (IL-GPE) have attracted much attention due to their good thermal stability and mechanical properties. Singh et al. studied imidazolyl ionic liquids and found that the EMIMFSI-based GPEs have excellent electrochemical stability, good compatibility and thermal stability (Singh et al., 2018). Guo et al. prepared the PVDF-HFP-LiTFSI/ $\text{SiO}_2$ /EMITFSI GPE with high thermal stability and good electrode compatibility (Guo et al., 2018). However, IL-GPE also has some shortcomings, such as lower

ionic conductivity and lithium ion mobility (Zhou et al., 2015). In this work, a piperidine ionic liquid, 1-methyl-1-propylpiperidinium chloride (PPCl), and  $\text{Li}_2\text{SiO}_3$  (LSO) nanoparticles were introduced into the PVDF-HFP matrix *via* coaxial electrospinning technology. The as prepared membrane has high porosity and electrolyte uptake, remarkable ionic conductivity, and outstanding electrochemical performance especially in quick charging. Commercial NCM622 cathode adopting this IL-GPE delivers a high reversible capacity of 65 mAh/g in 20C rate charge/discharge, which is 13 times higher than that of the cell adopting Celgard 2325 membrane.

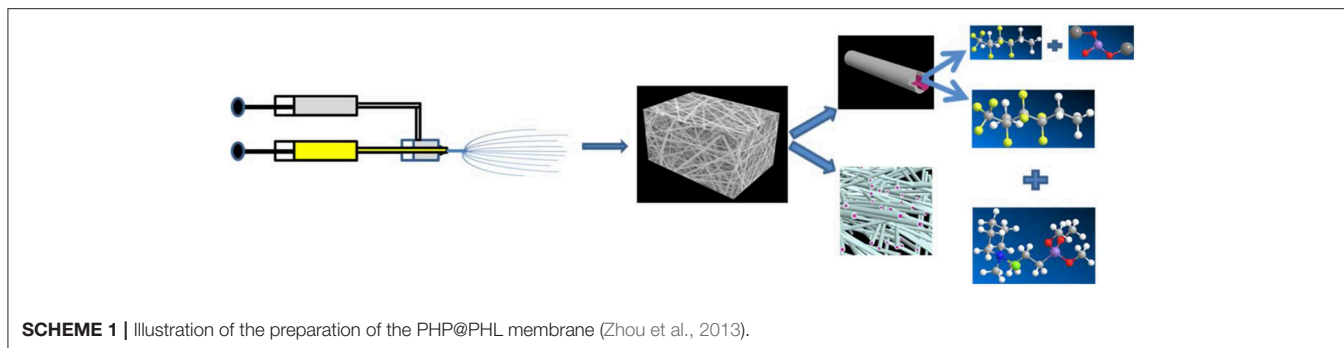
## EXPERIMENTAL SECTION

### Materials

Poly (vinylidene fluoride-co-hexafluoropropene) (PVDF-HFP, Mw.  $\sim 455,000$ ), 1-methylpiperidine (97%), and (3-chloropropyl) trimethoxysilane (98%) were provided by Sigma-Aldrich.  $\text{Li}_2\text{SiO}_3$  (LSO, 99%, Strem Chemicals), N, N-dimethylformamide (DMF, 99.5%, Beijing Chemical Works),  $\text{LiNi}_{0.6}\text{Co}_{0.2}\text{Mn}_{0.2}\text{O}_2$  (NCM622, Beijing Dangsheng Material Technology Co., Ltd.), Super P (Imerys Graphite & Carbon), Polyvinylidene difluoride (PVDF, Solvay 5130), N-Methyl-2-pyrrolidone (NMP, 99.0%, Sinopharm Chemical Reagent Co., Ltd.), lithium tablet (Li, Tianjin Zhongneng Co., Ltd.), and polypropylene (PP, Japan Ube) were commercially available and used without further purification.

### Preparation of the GPEs

The ionic liquid PPCl was synthesized according to the procedure reported before (Lu et al., 2012; Korf et al., 2014; Cheng et al., 2018), its structure and purity was also testified in our previous work (Xu et al., 2018). The core-shell structured 3D porous nanofiber membrane was prepared by the coaxial electrospinning technique on an ET-2535H machine (Ucalery Tech Inc., China), as shown in **Scheme 1**. To make composite nonwoven membrane, 80% (wt., similarly hereinafter) DMF was adopted in all the spinning solutions. The slurry for core spinning was prepared by mixing PPCl and PVDF-HFP in DMF solvent, wherein the weight ratio of PPCl: PVDF-HFP: DMF was fixed at 1:19:80. Correspondingly, the slurry for shell spinning was prepared by mixing LSO and PVDF-HFP in DMF solvent with a ratio of 2:18:80. The coaxial electrospinning equipment mainly contained a variable positive voltage of 15 kV and a negative voltage of  $-2\text{kV}$ , two syringe pumps, a spinneret consisting of two chambers and a collector. The pumped speed of the shell and core solutions supply were fixed at 0.25 and 0.15 mL/h, respectively, the distance between the needle tip and aluminum foil collector was 13 cm. The as prepared membrane has a thickness of  $50 \pm 5 \mu\text{m}$ , and was entitled by PHP@PHL. Accordingly, PVDF-HFP, PVDF-HFP-PPCl (PHP), and PVDF-HFP-LSO (PHL) nanofiber membrane was prepared by mixing PVDF-HFP in DMF (20:80), PPCl, and PVDF-HFP in DMF (1:19:80) or LSO and PVDF-HFP in DMF (2:18:80), respectively. The as-prepared nonwoven fiber membranes were cut into disc with a diameter of 16 mm, which were then dried in a vacuum oven at  $60^\circ\text{C}$  for 20 h to remove the residual solvent.



In the end, the membranes were filled and swollen in a liquid electrolyte, 1.2 M  $\text{LiPF}_6$  in ethylene carbonate (EC) and ethyl methyl carbonate (EMC) (3:7, weight ratio), for 30 min in an argon filled glove box to obtain the relevant GPEs.

## Characterization of the Membranes and GPEs

The thickness of various films was recorded by measuring membrane apparatus (CH1ST, Shanghai Milite Precise Instrument Co., Ltd., China), and morphology of the membrane was studied by field-emission scanning electron microscopy (FE-SEM, JSM-7001F, JEOL, Japan). The field emission transmission electron microscopy (TEM, JEOL, JEM-2100) was used to test the core-shell structure of PHP@PHL nanoporous fiber membrane. The surface chemical composition of PHP@PHL was analyzed by X-ray photoelectron spectroscopy (XPS, ESCALAB 250Xi, Thermo Fisher Scientific, America). Differential scanning calorimetry (DSC, Mettler-Toledo, Switzerland) was carried out to analyze the thermal behavior of all kinds of membranes. Samples were put into aluminum pans and the test temperature was set from 50 to 250°C with a heating rate of 5°C/min, under  $\text{N}_2$  atmosphere. The porosity of various films was measured by soaking n-butanol for 2 h, then calculated using Equation (1):  $P = (m_b/\rho_b)/(m_b/\rho_b + m_a/\rho_a) \times 100\%$ , where  $m_a$  and  $m_b$  are the weights of separators and n-butanol,  $\rho_a$  and  $\rho_b$  are the density of separators and n-butanol, respectively (Xiao et al., 2012; Zhou et al., 2013). In an argon filled glove box, the electrolyte uptakes were analyzed by the mass difference of separators before and after soaking in electrolyte for 30 min and then calculated using Equation (2):  $\text{EU} = (W - W_0)/W_0 \times 100\%$ , in which  $W_0$  and  $W$  are the weights of the films before and after immersing in the liquid electrolyte, respectively. Ten samples are tested to measure the electrolyte uptake and porosity of each membrane. Wettability of the separators were researched by contact angle measurements (DSA 100S, Germany KRUSS).

The various GPEs' effective ionic conductivities ( $\sigma$ ) were calculated using Equation (3):  $\sigma = d/(R_b \times S)$ , where  $d$  is the thickness of the film,  $S$  is the area and  $R_b$  is the bulk impedance acquired by electrochemical impedance spectroscopy (EIS) in Stainless Steel (SS)/electrolyte/SS symmetric cells. The bulk resistances ( $R_b$ ) were investigated by a CHI660E electrochemical workstation with a frequency range of 0.01–10<sup>5</sup> Hz and an amplitude of 5 mV at room temperature. The lithium ion transference numbers ( $t_{\text{Li}^+}$ ) of different electrolytes

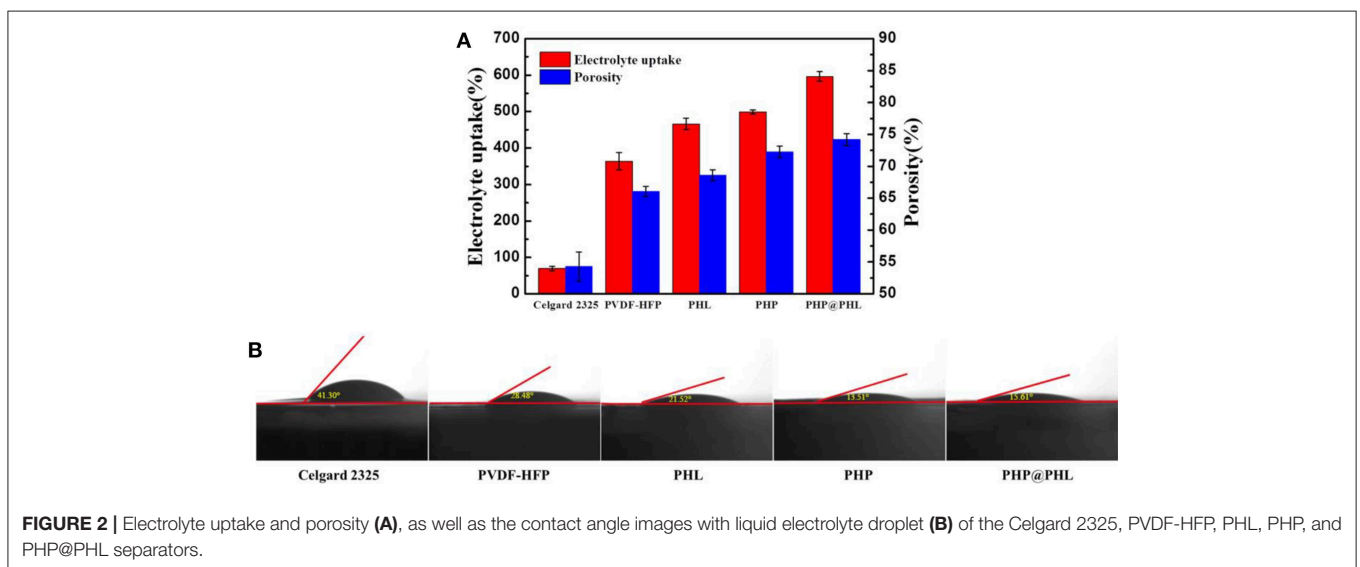
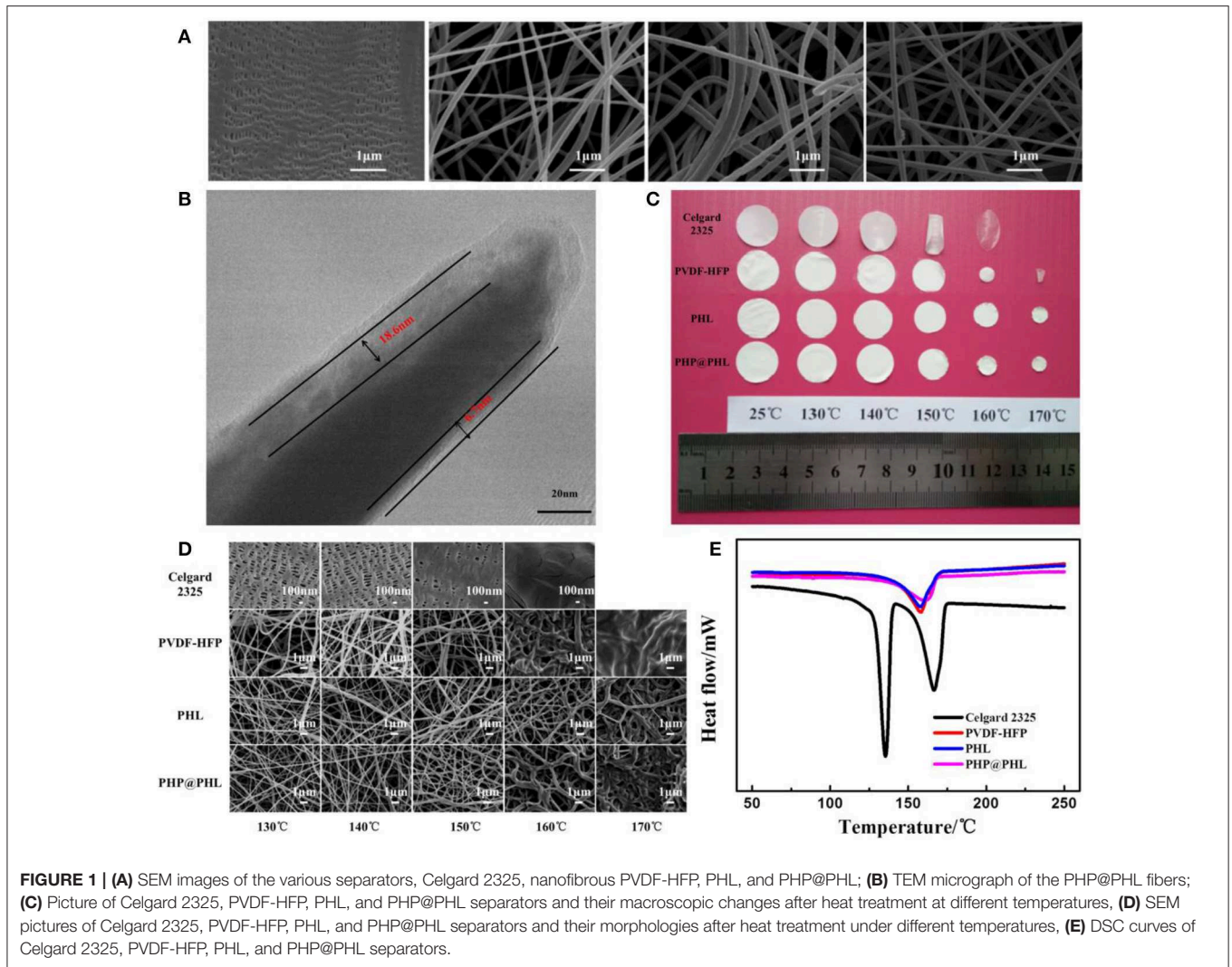
were tested using chronoamperometry (CA) and EIS (both by CHI660E), and then calculated using Equation (4):  $t_{\text{Li}^+} = I_S(\Delta V - I_0 R_0)/I_0(\Delta V - I_S R_S)$  (Li et al., 2018), where  $I_0$  and  $I_S$  are the initial and steady state currents obtained by CA testing of lithium symmetrical cell,  $R_0$  and  $R_S$  are the interfacial impedance before and after polarization, and  $\Delta V$  (10 mV) is the applied voltage difference (Yang et al., 2014; Zhang F. et al., 2014). The electrochemical performances were researched in coin cells with lithium foil anode and  $\text{LiNi}_{0.6}\text{Co}_{0.2}\text{Mn}_{0.2}\text{O}_2$  (NCM622) cathode. The interfacial stability between the electrode and electrolytes was investigated using EIS after standing for 1, 10, 20, and 30 days, respectively. The long term cycling stability, as well as rate performances were tested in a voltage range between 2.8 and 4.4 V with different C rates by LAND battery cycle system (Wuhan Blue Electric Co., LTD, China).

## RESULTS AND DISCUSSION

### Morphologies of the Membranes

The morphologies of the Celgard 2325 (which is a PP/PE/PP trilayer separator), nanofibrous PVDF-HFP, PHL, and PHP@PHL membranes, as well as microscopic changes after the thermal stability analyze in 130–170°C temperature range, were tested by using SEM, as shown in **Figures 1A,D**. The Celgard 2325 membrane has tensile holes in the lamellar matrix, but the electrostatic spinning films show 3D porous structure with 80–160 nm diameter nanofiber which interlacing with each other to form interconnected networks. The energy dispersive X-ray spectroscopy (EDS) data shown in **Figure S1** gives the elemental distribution in PHL and PHP@PHL complex films. As shown in **Figure S1a**, Si and O are uniformly distributed in the membrane, which proves that  $\text{Li}_2\text{SiO}_3$  is evenly dispersed in the polymer matrix. EDS results of PHP@PHL in **Figure S1b** shows little signal of N or Cl as the content of PPCL is pretty low (<2%). TEM image of PHP@PHL nanofiber further proved its core-shell structure, and the inorganic nanoparticle  $\text{Li}_2\text{SiO}_3$  is dispersed in the out layer of the PVDF-HFP matrix, with the thickness of several to tens of nanometers as shown in **Figure 1B**. The XPS spectra in **Figure S2** detected no Cl element on the surface of PHP@PHL nanofiber, which further proves that the PPCL ionic liquid was fully encapsulated by the out PHL layer.

The thermal stability of various membranes was investigated by storing them in an air circulation oven at a series of temperatures between 130 and 170°C, each for 20 min. **Figure 1C**



shows that Celgard 2325 begins to curl for the melting of PE and molecular tanglement of polyolefin at about 135°C, it turns transparent at 160°C for the melt of PP, meanwhile PVDF-HFP shrink at 150°C and melt at 170°C. However, the PHL and PHP@PHL keeps their porous structure even at 170°C. It can be concluded that the inorganic nano-particle,  $\text{Li}_2\text{SiO}_3$ , in the shell structure significantly improved the thermal stability of the separator, which may potentially contribute in enhancing the safety of the battery. In order to further clarify the morphology changes of the films after heat treatment, FE-SEM pictures of the four separators are given in **Figure 1D** for microscopic description. Celgard 2325 was fully shutdown at 160°C, and PVDF-HFP nanofibrous films melt under 170°C, but the PHL and PHP@PHL films still keeps certain amount of pores remain in 170°C (**Figure 1D**). From the microscopic point of view, the core-shell structure nanofibrous membrane expresses excellent thermal stability, hence makes it have distinguished heat resistance and advance the safety of lithium battery under high temperature condition. According to DSC test results of four separators, membranes based on PVDF-HFP shows better thermal stability than that of Celgard 2325, and the core-shell structured PHP@PHL, released the least heat even on melting (**Figure 1E**) (Kang et al., 2016; Wang et al., 2019).

Porosity of the membranes are tested and calculated by Equation (1) as shown in **Figure 2A**, it's about 54.4, 66.1, 68.5, 72.5, and 74.0% for Celgard 2325, PVDF-HFP, PHL, PHP, and PHP@PHL, respectively. Obviously, fibrous separators have higher porosity than Celgard 2325, which may contribute in electrolyte uptake and thus enhance the rate capability. Contact angle of liquid electrolyte to various membranes were also studied and shown in **Figure 2B**. The contact angle of Celgard 2325, PVDF-HFP, PHL, PHP and PHP@PHL is 41.30, 28.48, 21.52, 13.51, and 15.61°, respectively. All fibrous

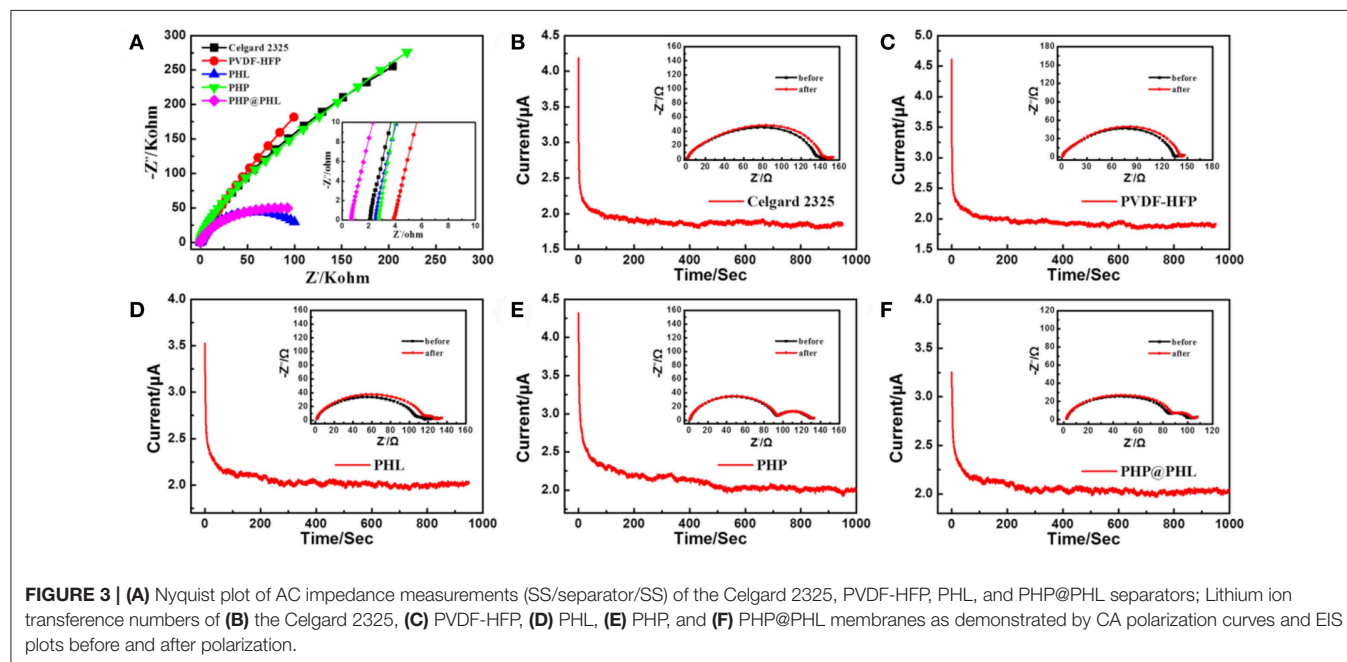
membranes showed smaller contact angle with electrolyte for the high dielectric constant of PVDF-HFP (Lopez et al., 2018), besides, they also beneficial from the fibrous structure. Smaller contact angle indicated that the PHP@PHL composite nanofibrous membrane has better affinity and is easier to be wetted by the liquid electrolyte, thus better rate capability might be obtained.

The effect ionic conductivity of the five separators was probed by EIS test at ambient temperature and calculated by Equation (3) as shown in **Figure 3A**.  $R_b$  obtained from EIS data is 2.1105, 3.8473, 2.5165, 3.3936, and 0.6801  $\Omega$  for Celgard 2325, PVDF-HFP, PHL, PHP, and PHP@PHL, respectively, and the corresponding effect ionic conductivity are 0.63, 0.64, 1.03, 1.02, and 4.05 mS/cm, respectively. Consistent with the results of porosity and wettability, this data further guaranteed the enhanced rate capability in cells.

The lithium ion transference number ( $t_{\text{Li}^+}$ ) of Celgard 2325 and the as-prepared membranes with liquid electrolyte was tested and calculated via Equation (4) as shown in **Figures 3B–F**, where the corresponding  $t_{\text{Li}^+}$  are 0.42, 0.39,

**TABLE 1** | The film thickness, electrolyte uptake, porosity, effective ionic conductivity, and lithium ion transference number of Celgard 2325, PVDF-HFP, PHL, PHP, and PHP@PHL separators.

	Films thickness ( $\mu\text{m}$ )	Electrolyte uptake (%)	Porosity (%)	Conductivity ( $\text{mS cm}^{-1}$ )	$t_{\text{Li}^+}$
Celgard 2325	25 $\pm$ 1	70 $\pm$ 3	54.4 $\pm$ 1.1	0.63	0.42
PVDF-HFP	50 $\pm$ 5	366 $\pm$ 12	66.1 $\pm$ 0.4	0.64	0.39
PHL	50 $\pm$ 5	466 $\pm$ 8	68.5 $\pm$ 0.4	1.03	0.56
PHP	50 $\pm$ 5	498 $\pm$ 3	72.5 $\pm$ 0.5	1.02	0.45
PHP@PHL	50 $\pm$ 5	597 $\pm$ 8	74.0 $\pm$ 0.5	4.05	0.62



0.56, 0.45, and 0.62, respectively.  $t_{Li^+}$  reduced from 0.42 to 0.39 when Celgard 2325 was replaced by PVDF-HFP, which proves that the polymer itself in fact has little contribute in  $Li^+$  transference. The addition of  $Li_2SiO_3$  enhanced the number to 0.56, which demonstrated that the inorganic nanoparticle may facilitate the desolvation of  $Li^+$ . While  $t_{Li^+}$  of PHP is only 0.45, slightly higher than that of Celgard 2325 and PVDF-HFP, the reason lays on that although PPCI was mixed with PVDF-HFP and formed a membrane, but the Cl anion could still partly dissociated into the electrolyte thus influence the transportation of  $Li^+$  (Xu et al., 2018). PHP@PHL shows the highest  $t_{Li^+}$  among the five electrolytes for the synergistic effect of LSO and PPCI, encapsulated by the PHL layer, the Cl anion could not influence the  $Li^+$  transport but adjust the polarization of the separator polymer matrix. Therefore, PHP@PHL nanofiber membrane prominently improves the  $t_{Li^+}$ , which may contribute in reduces anion aggregation near the electrode surface, thus reduces the concentration polarization and stabilizes the electrochemical deposition of lithium ions, improving the safety of LIB.

The film thickness, electrolyte uptake, porosity, ionic conductivity, and lithium ion transference number of the Celgard 2325, PVDF-HFP, PHL, and PHP@PHL separators summarized in Table 1. It is worth noting that the electrolyte uptake of PHP@PHL was about 597%, which is much higher than

that of Celgard 2325 (70%), PVDF-HFP (366%), PHL (466%), and PHP (498%) and further contribute in the better rate capability when adopting in the LIBs. PHP@PHL composite membrane demonstrated the highest porosity and electrolyte uptake ability, the smallest electrolyte contact angle, and there are several factors that contribute to its remarkable performances. Firstly, the molecular structure of PVDF-HFP, as well as the 3D nanofibrous morphology facilitated the electrolyte uptake, for its high polarity and the nanoporous structure. Secondly,  $Li_2SiO_3$  and PPCI reduced the order of molecular arrangement, which produced more chances for the electrolyte to be taken. Moreover, PPCI also worked as a plasticizer which has perfect affinity with the electrolyte, on which the contact angle is also reduced. Therefore, PHP@PHL shows the best physical performances. We also compare the ionic conductivity and the  $t_{Li^+}$  with some of the previous publications as listed in Table 2, obviously, by the synergistic effect of LSO and PPCI, lithium ion transport efficiency was strongly enhanced.

Galvanostatic cycling measurements in Li/electrolyte/Li symmetrical cells can probed into lithium plating/stripping process and analyze the interfacial stability between the electrolyte and lithium electrode. The charge/discharge cycling test was performed at a fixed current density of  $0.5 \text{ mA/cm}^2$  with a total capacity of  $1 \text{ mAh/cm}^2$  and the results are shown in Figure 4. As can be seen from the Celgard 2325 voltage-time profile, it exhibits a gradual increase in hysteresis (overpotential between Li deposition and dissolution) as the time increases, and the voltage increases to 0.65 V after 300 h. In other words, the SEI film, or dead lithium is thickening with cycling, which means an out-of-balance lithium plating/stripping. The voltage-time profiles of PVDF-HFP, PHL, and PHP@PHL electrolytes were much stable compared with that of Celgard 2325. In particular, although the  $t_{Li^+}$  of PVDF-HFP is lower than that of Celgard 2325, while it turns quite stable in the initial 500 h owing to the fibrous structure of the membrane which could balance the  $Li^+$  flux adjacent to the electrode. PHL presents the least hysteresis after 1,000 h plating/stripping, while as it shows several abnormal convex during the cycling, therefore, we consider that the PHP@PHL cell demonstrated the best stability. As discussed before, the enhanced performance of PHP@PHL can be attributed to several reasons, firstly, the

TABLE 2 | Ionic conductivity and  $t_{Li^+}$  in previous relevant works.

Type of GPE	Conductivity $\sigma$ (mS/cm)	$t_{Li^+}$	References
PVDF-HFP@ $Al_2O_3$ GPE	1.24	–	Shen et al., 2018
40 wt% IL GPE	0.15	0.39	Singh et al., 2018
PSA@PVDF-HFP	1.97	–	Zhou et al., 2013
PMMA/PVDF-HFP	1.31	–	Zhang J. et al., 2014
MS5 based GPE	3.2	0.62	Li et al., 2018
Gel PVDF-NWF	0.3	–	Zhu et al., 2013
$SiO_2@Li^+$ doped PVDF-HFP	3.9	0.44	Xiao et al., 2012
NanoIL GPE	0.64	0.6	Cheng et al., 2018
PHP@PHL	4.05	0.62	This work

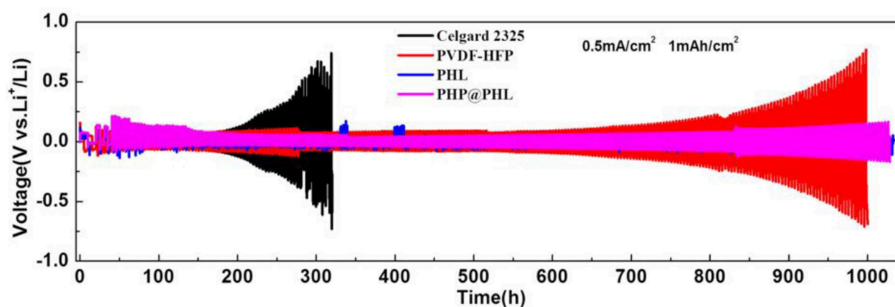
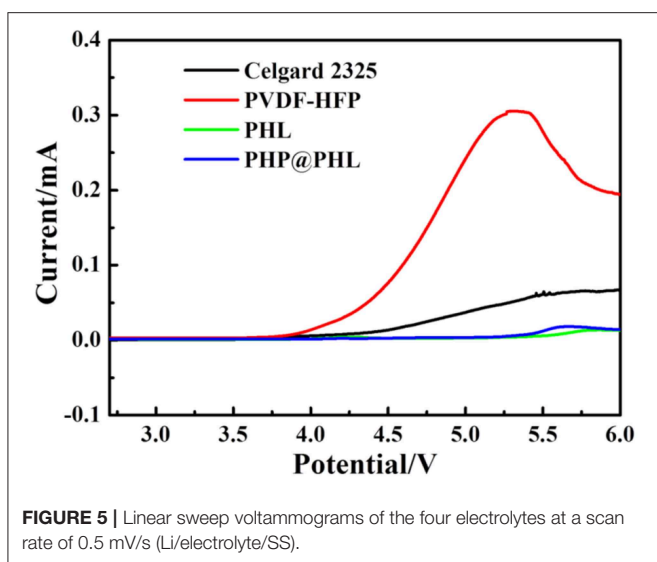


FIGURE 4 | Galvanostatic cycling performances of symmetric lithium cells with the Celgard 2325, PVDF-HFP, PHL, and PHP@PHL separators at a current density of  $0.5 \text{ mA/cm}^2$  at  $25^\circ\text{C}$ .



nanofibrous structure of PVDF-HFP balanced the  $\text{Li}^+$  flux and suppressed the mossy deposition of Li; secondly, the synergistic effect of LSO and PPCI reduce the crystallinity of the polymer matrix, thus enhanced the  $\text{Li}^+$  transportation efficiency; lastly, Cl anion from the IL may partly be involved in the formation of SEI, which further enhance the cycle stability of the symmetric cell. Hence, the formation of Li dendrites is inhibited and the speed of dendrite growth is reduced as well. These results manifest that using 3D porous electrostatic spinning nanofiber membrane could effectively lower the hysteresis, stabilize cycling behavior and elongate the cell lifetime.

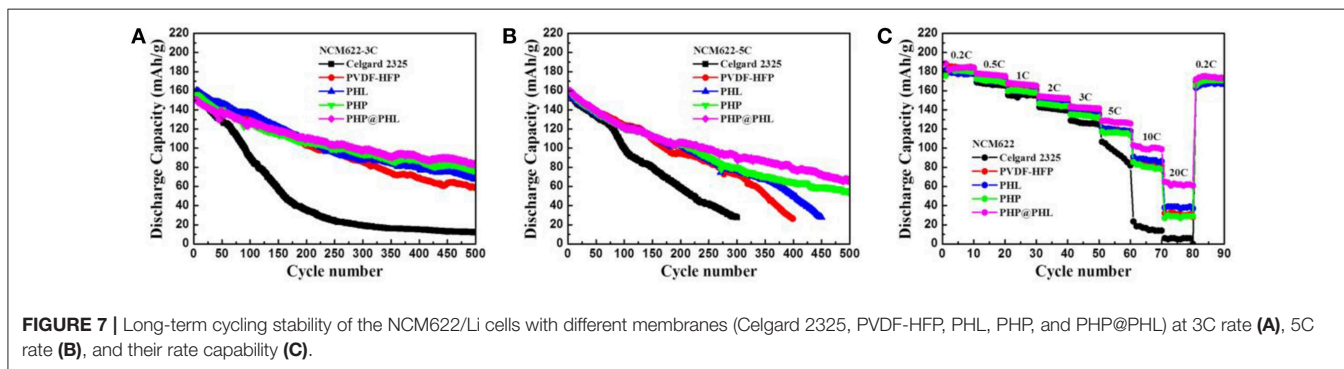
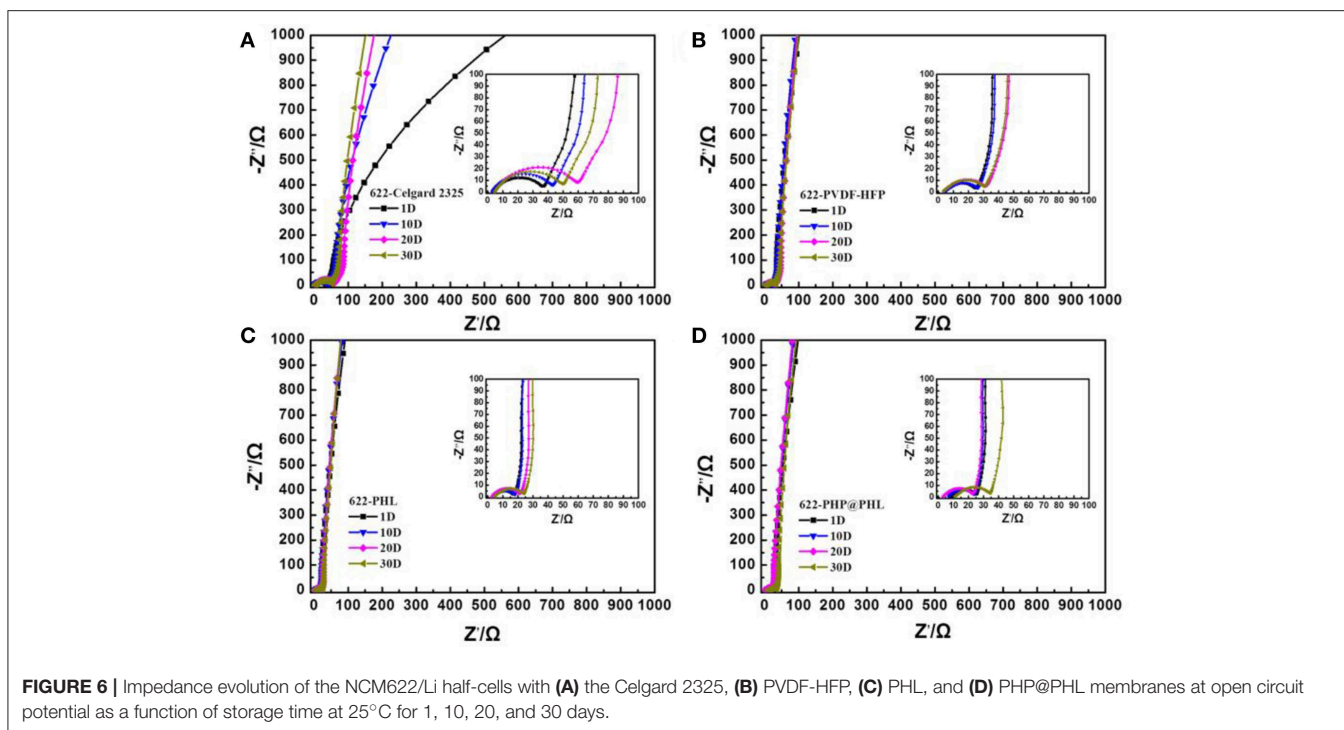
The batteries tested with the above four electrolytes were then disassembled in an argon-protected glove box, the electrodes were cleaned with diethyl carbonate (DEC) and dried strictly, and then put into a vacuum transfer box before FE-SEM analysis. The experimental results are shown in **Figure S3**. For the symmetrical lithium battery assembled with Celgard 2325 after galvanostatic charge/discharge cycle for 300 h, the FE-SEM diagram indicates that a lot of clavate-shaped lithium dendrite is generated on the surface of the lithium electrode. These dendrites will eventually penetrate the separator, causing short circuit and safety problems. By contrast, the symmetrical lithium battery assembled with the electrostatic spinning films, PVDF-HFP, PHL, and PHP@PHL, even cycled for 1,000 h under the same current density, shows much smoother surface with smooth edges, which was not easy to penetrate the separators, greatly improved the safety of LIBs. The electrospinning separators have large specific surface area, which could balance the local current density on the electrode surface, thus inhibited the formation and growth of lithium dendrite. Therefore, the core-shell nanofiber separator prepared by coaxial electrostatic spinning can significantly improve the safety performance of LIB.

Linear sweep voltammetry (LSV) was used to investigate the electrochemical windows of the electrolytes with a scan rate of 0.5 mV/s over the range of 2.8–6 V in Li/electrolyte/SS

battery, and the results are shown in **Figure 5**. The oxidation potentials of the Celgard 2325, PVDF-HFP, PHL, and PHP@PHL electrolyte is 4.27, 3.93, 5.5, and 5.45 V (vs.  $\text{Li}^+/\text{Li}$ ), respectively. As all these membranes are plasticized by the same electrolyte,  $\text{LiPF}_6/\text{EC}+\text{EMC}$ , therefore, most parasitic reactions should origin from the membrane. Therefore, it can be concluded that both LSO and PPCI could prevent PVDF-HFP from being oxidized and effectively enhance the electrochemical stability of composite membrane, which is pivotal for practical application. No obvious decomposition of Li/PHP@PHL/SS battery was observed below 5.45 V, which manifested PHP@PHL may potentially be able to be coupled with high voltage cathode materials, such as NCM622.

The interfacial stability between the electrode and the electrolyte is fatal for long-term cycle stability and rate performance, therefore, the separators are adopted and Li/electrolyte/NCM622 half-cells were assembled to further test their compatibility with the electrode materials. Static EIS tests were performed in 1, 10, 20, and 30 days after cell assembled at room temperature and the data was deal with an equivalent circuit fitting (**Figure S4**), the results are shown in **Figure 6** and **Table S1**.  $R_b$  is corresponding to the bulk resistance originated from electrolyte and other cell components,  $R_1$  and  $R_2$  can be assigned to the interface resistance between electrolyte and anode or cathode, respectively.  $R_2$  is smaller than  $R_1$  because the battery is never charged after assembly and is left standing, therefore, little reaction would happen in the storage process. The cell with PHP@PHL shows the most stable  $R_1$  value among the four cells, it is 18.32  $\Omega$  after 30 days of storage, while it is 61.40, 35.45, and 35.42  $\Omega$  for Celgard 2325, PVDF-HFP and PHL, respectively, which indicates that PHP@PHL has the best interfacial compatibility with Li among these electrolytes (Cheng et al., 2018). Its smallest increase in interface resistance is mainly attributed to the following reason: firstly, PVDF-HFP has higher dielectric constant than PP or PE, which endows it with better Li compatibility (Lopez et al., 2018); secondly, the introduction of  $\text{Li}_2\text{SiO}_3$  partially suppresses the decomposition of  $\text{LiPF}_6$  and carbonate solvents during long term storage (Fu et al., 2017); and the third, the slow dissociation of PPCI would generate some Cl anion, which would react with Li to form a more stable SEI component, LiCl, thus further stabilized the electrode/electrolyte interface and reduce its resistance (Lu et al., 2014b).

Electrochemical performances of the above mentioned GPEs were tested in Li/electrolyte/NCM622 half cells by different C rates. **Figure S5** shows the 0.5C rate performance of Celgard 2325 and PHP@PHL, we can see that the cells delivers quite similar capacity in the initial 300 cycles, both cells kept more than 100 mAh/g reversible capacity in 500 cycles, which proves that the cathode material works well in this electrolyte system. It also can be notice that the Celgard one shows lower coulombic efficiency after about 350 cycles, which might cause by the mossy Li deposition after long term stripping/plating. High rate tests were performed to testify the performance of nanofibrous GPEs. **Figures 7A,B** show the long term cycle performances of the Li/electrolyte/NCM622 half cells at 3C and



5C, respectively. Obviously, the reversible capacity and cycle stability of PHP@PHL system were significantly improved at these C rates. The initial discharge capacities of Celgard 2325, PVDF-HFP, PHL, PHP, and PHP@PHL were 156.6, 160.6, 161.4, 156.5, and 150.6 mAh/g at 3C rate, respectively. It drops sharply to 15.8 mAh/g after 300 cycles for the Celgard 2325 one, while that of PVDF-HFP, PHL, PHP, and PHP@PHL maintained at 85.3, 87.9, 84.1, and 98.5 mAh/g, respectively. The initial discharge capacities of Celgard 2325, PVDF-HFP, PHL, PHP, and PHP@PHL at 5C rate were 156.0, 156.0, 156.2, 158.7, and 160.2 mAh/g, respectively. It declined dramatically to 27.8 mAh/g after 300 cycles for Celgard 2325, and that of PVDF-HFP and PHL were also significantly reduced to 26.3 and 27.2 mAh/g after 400 cycles, respectively. But the one with PHP@PHL remained 78.5 mAh/g even after 500 cycles. The rate performances (from 0.2 to 20C) of Li/electrolyte/NCM622 half-cells are shown

in **Figure 7C**. It can be seen that the difference between the electrospinning GPEs and the Celgard separator was not obvious under low current density, but the diversity significantly improved under large current density, especially for PHP@PHL. The Li/electrolyte/NCM622 half-cell with PHP@PHL can still deliver a reversible capacity of 65 mAh/g at 20C, while that of Celgard 2325, PVDF-HFP, PHL, and PHP were 5, 30, 38, and 29 mAh/g, respectively, which means the PHP@PHL delivers 13 times higher capacity than that of Celgard 2325. Charge-discharge profiles of the Li/electrolyte/NCM622 half-cells with Celgard 2325 and PHP@PHL at different C rates were compared in **Figure S6**. It can be easily conclude from these results that the as prepared core-shell structure PHP@PHL nanofibrous electrolyte has the best electrochemical performances, which can realize safe and efficient quick charging, thus has great potential in the application of high-power density LIBs.

## CONCLUSIONS

In summary, a core-shell structured nanofibrous membrane with PPhCl ionic liquid plasticizer in the core and inorganic nano-particle  $\text{Li}_2\text{SiO}_3$  as the filler in shell, PHP@PHL, was prepared by a facile coaxial electrospinning method. The electrolyte uptake, porosity, ionic conductivity and lithium ion transference number of PHP@PHL nanofiber membrane were about 597%, 74.0%, 4.05 mS/cm, and 0.62, respectively. By the introduction of PPhCl and  $\text{Li}_2\text{SiO}_3$ , ionic conductivity of the electrolyte increases by an order of magnitude and wettability between the separator and liquid electrolyte also significantly improved compared to commercial Celgard 2325 or even electrospinning PVDF-HFP separator. In addition, it has good thermal stability, low interfacial impedance and wide electrochemical window. Symmetrical lithium cells with PHP@PHL demonstrated excellent plating/stripping cycling stability for about 1,000 h without short-circuit, which is 5 times longer than that of Celgard 2325. Moreover, the PHP@PHL electrolyte presents outstanding rate capability, it delivers a reversible capacity of 65 mAh/g at 20C compared to the 5 mAh/g in the case of Celgard 2325. The long term cycle performance was also significantly improved, as demonstrated in 3C and 5C. The core-shell structured nanofibrous membrane, in which different fillers or plasticizers could be used thus different functions can be realized in one single membrane, provides an effective method to enhance the overall performances of LIBs.

## REFERENCES

- Ali, S., Tan, C., Waqas, M., Lv, W., Wei, Z., Wu, S., et al. (2018). Highly efficient PVDF-HFP/colloidal alumina composite separator for high-temperature lithium-ion batteries. *Adv. Mater. Interfaces* 5:1701147. doi: 10.1002/admi.201701147
- Chen, N., Dai, Y., Xing, Y., Wang, L., Guo, C., Chen, R., et al. (2017). Biomimetic ant-nest ionogel electrolyte boosts the performance of dendrite-free lithium batteries. *Energy Environ. Sci.* 10, 1660–1667. doi: 10.1039/C7EE00988G
- Cheng, Y., Zhang, L., Xu, S., Zhang, H., Ren, B., Li, T., et al. (2018). Ionic liquid functionalized electrospun gel polymer electrolyte for use in a high-performance lithium metal battery. *J. Mater. Chem. A* 6, 18479–18487. doi: 10.1039/C8TA06338A
- Choi, S. W., Jo, S. M., Lee, W. S., and Kim, Y. R. (2003). An electrospun poly(vinylidene fluoride) nanofibrous membrane and its battery applications. *Adv. Mater.* 15, 2027–2032. doi: 10.1002/adma.200304617
- Deng, K., Qin, J., Wang, S., Ren, S., Han, D., Xiao, M., et al. (2018). Effective suppression of lithium dendrite growth using a flexible single-ion conducting polymer electrolyte. *Small* 14:e1801420. doi: 10.1002/smll.201801420
- Diederichsen, K. M., McShane, E. J., and McCloskey, B. D. (2017). Promising routes to a high  $\text{Li}^+$  transference number electrolyte for lithium ion batteries. *ACS Energy Lett.* 2, 2563–2575. doi: 10.1021/acsenenergylett.7b00792
- Etacheri, V., Marom, R., Elazari, R., Salitra, G., and Aurbach, D. (2011). Challenges in the development of advanced Li-ion batteries: a review. *Energy Environ. Sci.* 4, 3243–3262. doi: 10.1039/c1ee01598b
- Fu, J., Mu, D., Wu, B., Bi, J., Liu, X., Peng, Y., et al. (2017). Enhanced electrochemical performance of  $\text{LiNi}_{0.6}\text{Co}_{0.2}\text{Mn}_{0.2}\text{O}_2$  cathode at high cutoff voltage by modifying electrode/electrolyte interface with lithium metasilicate. *Electrochim. Acta* 246, 27–34. doi: 10.1016/j.electacta.2017.06.038
- Gao, Y., Shan, D. C., Cao, F., Gong, J., Li, X., Ma, H. Y., et al. (2009). Silver/polyaniline composite nanotubes: one-step synthesis and electrocatalytic

## DATA AVAILABILITY

The raw data supporting the conclusions of this manuscript will be made available by the authors, without undue reservation, to any qualified researcher.

## AUTHOR CONTRIBUTIONS

SZ helps to improve ideas and experimental platform. LZ helps to solve some problems of experience. XL helps to do mainly works. YR helps to do any experience.

## FUNDING

This work was financially supported by the National Key Research and Development Program of China (No. 2016YFB0100303), National Natural Science Foundation of China (No. 21706261), Beijing Natural Science Foundation (No. L172045), and the Ford-China University Research Program.

## SUPPLEMENTARY MATERIAL

The Supplementary Material for this article can be found online at: <https://www.frontiersin.org/articles/10.3389/fchem.2019.00421/full#supplementary-material>

activity for neurotransmitter dopamine. *J. Phys. Chem. C* 113, 15175–15181. doi: 10.1021/jp904788d

- Ghazi, Z. A., He, X., Khattak, A. M., Khan, N. A., Liang, B., Iqbal, A., et al. (2017).  $\text{MoS}_2$ /celgard separator as efficient polysulfide barrier for long-life lithium-sulfur batteries. *Adv. Mater.* 29:1606817. doi: 10.1002/adma.201606817
- Goodenough, J. B., and Kim, Y. (2010). Challenges for rechargeable Li batteries. *Chem. Mater.* 22, 587–603. doi: 10.1021/cm901452z
- Guo, Q., Han, Y., Wang, H., Xiong, S., Liu, S., Zheng, C., et al. (2018). Preparation and characterization of nanocomposite ionic liquid-based gel polymer electrolyte for safe applications in solid-state lithium battery. *Solid State Ionics* 321, 48–54. doi: 10.1016/j.ssi.2018.03.032
- Huang, X. (2010). Separator technologies for lithium-ion batteries. *J. Solid State Electr.* 15, 649–662. doi: 10.1007/s10008-010-1264-9
- Jana, A., Ely, D. R., and García, R. E. (2015). Dendrite-separator interactions in lithium-based batteries. *J. Power Sources* 275, 912–921. doi: 10.1016/j.jpowsour.2014.11.056
- Jia, H., Onishi, H., Wagner, R., Winter, M., and Cekic-Laskovic, I. (2018). Intrinsically safe gel polymer electrolyte comprising flame-retarding polymer matrix for lithium ion battery application. *ACS Appl. Mater. Interfaces* 10, 42348–42355. doi: 10.1021/acsmi.8b15505
- Kang, W., Deng, N., Ma, X., Ju, J., Li, L., Liu, X., et al. (2016). A thermostability gel polymer electrolyte with electrospun nanofiber separator of organic F-doped poly-m-phenyleneisophthalamide for lithium-ion battery. *Electrochim. Acta* 216, 276–286. doi: 10.1016/j.electacta.2016.09.035
- Kim, S., Han, T., Jeong, J., Lee, H., Ryou, M.-H., and Lee, Y. M. (2017). A flame-retardant composite polymer electrolyte for lithium-ion polymer batteries. *Electrochim. Acta* 241, 553–559. doi: 10.1016/j.electacta.2017.04.129
- Kim, Y. B., Tran-Phu, T., Kim, M., Jung, D. W., Yi, G. R., and Park, J. H. (2015). Facilitated ion diffusion in multiscale porous particles: application in battery separators. *ACS Appl. Mater. Interfaces* 7, 4511–4517. doi: 10.1021/am506797d

- Korf, K. S., Lu, Y., Kambe, Y., and Archer, L. A. (2014). Piperidinium tethered nanoparticle-hybrid electrolyte for lithium metal batteries. *J. Mater. Chem. A* 2, 11866–11873. doi: 10.1039/C4TA02219J
- Lee, H., Yanilmaz, M., Toprakci, O., Fu, K., and Zhang, X. (2014). A review of recent developments in membrane separators for rechargeable lithium-ion batteries. *Energy Environ. Sci.* 7, 3857–3886. doi: 10.1039/C4EE01432D
- Li, M., Liao, Y., Liu, Q., Xu, J., Sun, P., Shi, H., et al. (2018). Application of the imidazolium ionic liquid based nano-particle decorated gel polymer electrolyte for high safety lithium ion battery. *Electrochim. Acta* 284, 188–201. doi: 10.1016/j.electacta.2018.07.140
- Li, Q., Chen, D., Tan, H., Zhang, X., Rui, X., and Yu, Y. (2019). 3D porous V<sub>2</sub>O<sub>5</sub> architectures for high-rate lithium storage. *J. Energy Chem.* 40, 15–21. doi: 10.1016/j.jechem.2019.02.010
- Liang, H.-q., Wan, L.-s., and Xu, Z.-k. (2016). Poly(vinylidene fluoride) separators with dual-asymmetric structure for high-performance lithium ion batteries. *Chin. J. Polym. Sci.* 34, 1423–1435. doi: 10.1007/s10118-016-1860-y
- Liu, K., Bai, P., Bazant, M. Z., Wang, C.-A., and Li, J. (2017a). A soft non-porous separator and its effectiveness in stabilizing Li metal anodes cycling at 10 mA cm<sup>-2</sup> observed *in situ* in a capillary cell. *J. Mater. Chem. A* 5, 4300–4307. doi: 10.1039/C7TA00069C
- Liu, K., Zhuo, D., Lee, H.-W., Liu, W., Lin, D., Lu, Y., et al. (2017b). Extending the life of lithium-based rechargeable batteries by reaction of lithium dendrites with a novel silica nanoparticle sandwiched separator. *Adv. Mater.* 29:1603987. doi: 10.1002/adma.201603987
- Lopez, J., Pei, A., Oh, J. Y., Wang, G. N., Cui, Y., and Bao, Z. (2018). Effects of polymer coatings on electrodeposited lithium metal. *J. Am. Chem. Soc.* 140, 11735–11744. doi: 10.1021/jacs.8b06047
- Lu, Q., He, Y. B., Yu, Q., Li, B., Kaneti, Y. V., Yao, Y., et al. (2017). Dendrite-free, high-rate, long-life lithium metal batteries with a 3D cross-linked network polymer electrolyte. *Adv. Mater.* 29:1604460. doi: 10.1002/adma.201604460
- Lu, Y., Korf, K., Kambe, Y., Tu, Z., and Archer, L. A. (2014a). Ionic-liquid-nanoparticle hybrid electrolytes: applications in lithium metal batteries. *Angew. Chem. Int. Edit.* 53, 488–492. doi: 10.1002/anie.201307137
- Lu, Y., Moganty, S. S., Schaefer, J. L., and Archer, L. A. (2012). Ionic liquid-nanoparticle hybrid electrolytes. *J. Mater. Chem.* 22, 4066–4072. doi: 10.1039/c2jm15345a
- Lu, Y., Tu, Z., and Archer, L. A. (2014b). Stable lithium electrodeposition in liquid and nanoporous solid electrolytes. *Nat. Mater.* 13, 961–969. doi: 10.1038/nmat4041
- Lu, Y., Tu, Z., Shu, J., and Archer, L. A. (2015a). Stable lithium electrodeposition in salt-reinforced electrolytes. *J. Power Sources* 279, 413–418. doi: 10.1016/j.jpowsour.2015.01.030
- Lu, Y., Xu, S., Shu, J., Aladat, W. I. A., and Archer, L. A. (2015b). High voltage LIB cathodes enabled by salt-reinforced liquid electrolytes. *Electrochem. Commun.* 51, 23–26. doi: 10.1016/j.elecom.2014.11.010
- Ma, X., Kolla, P., Yang, R., Wang, Z., Zhao, Y., Smirnova, A. L., et al. (2017). Electrospun polyacrylonitrile nanofibrous membranes with varied fiber diameters and different membrane porosities as lithium-ion battery separators. *Electrochim. Acta* 236, 417–423. doi: 10.1016/j.electacta.2017.03.205
- Park, S.-R., Jung, Y.-C., Shin, W.-K., Ahn, K. H., Lee, C. H., and Kim, D.-W. (2017). Cross-linked fibrous composite separator for high performance lithium-ion batteries with enhanced safety. *J. Membrane Sci.* 527, 129–136. doi: 10.1016/j.memsci.2017.01.015
- Rui, X., Tang, Y., Malyi, O. I., Gusak, A., Zhang, Y., Niu, Z., et al. (2016). Ambient dissolution–recrystallization towards large-scale preparation of V<sub>2</sub>O<sub>5</sub>nanobelts for high-energy battery applications. *Nano Energy* 22, 583–593. doi: 10.1016/j.nanoen.2016.03.001
- Scrosati, B., Hassoun, J., and Sun, Y.-K. (2011). Lithium-ion batteries. A look into the future. *Energy Environ. Sci.* 4, 3287–3295. doi: 10.1039/c1ee01388b
- Shen, X., Li, C., Shi, C., Yang, C., Deng, L., Zhang, W., et al. (2018). Core-shell structured ceramic nonwoven separators by atomic layer deposition for safe lithium-ion batteries. *Appl. Surf. Sci.* 441, 165–173. doi: 10.1016/j.apsusc.2018.01.222
- Shin, W. K., Kannan, A. G., and Kim, D. W. (2015). Effective suppression of dendritic lithium growth using an ultrathin coating of nitrogen and sulfur codoped graphene nanosheets on polymer separator for lithium metal batteries. *ACS Appl. Mater. Inter.* 7, 23700–23707. doi: 10.1021/acsami.5b07730
- Singh, S. K., Shalu, B. L., Gupta, H., Singh, V. K., Tripathi, A. K., and Singh, R. K. (2018). Improved electrochemical performance of EMIMFSI ionic liquid based gel polymer electrolyte with temperature for rechargeable lithium battery. *Energy* 150, 890–900. doi: 10.1016/j.energy.2018.03.024
- Sun, G., Dong, G., Kong, L., Yan, X., Tian, G., Qi, S., et al. (2018). Robust polyimide nanofibrous membrane with porous-layer-coated morphology by *in situ* self-bonding and micro-crosslinking for lithium-ion battery separator. *Nanoscale* 10, 22439–22447. doi: 10.1039/C8NR07548D
- Tan, H., Xu, L., Geng, H., Rui, X., Li, C., and Huang, S. (2018). Nanostructured Li<sub>3</sub>V<sub>2</sub>(PO<sub>4</sub>)<sub>3</sub> cathodes. *Small* 14:e1800567. doi: 10.1002/smll.201800567
- Tarascon, J. M., and Armand, M. (2001). Issues and challenges facing rechargeable lithium batteries. *Nature* 414, 359–367. doi: 10.1038/35104644
- Varzi, A., Raccichini, R., Passerini, S., and Scrosati, B. (2016). Challenges and prospects of the role of solid electrolytes in the revitalization of lithium metal batteries. *J. Mater. Chem. A* 4, 17251–17259. doi: 10.1039/C6TA07384K
- Wang, L., Deng, N., Ju, J., Wang, G., Cheng, B., and Kang, W. (2019). A novel core-shell structured poly-m-phenyleneisophthalamide@polyvinylidene fluoride nanofiber membrane for lithium ion batteries with high-safety and stable electrochemical performance. *Electrochim. Acta* 300, 263–273. doi: 10.1016/j.electacta.2019.01.115
- Wang, M., Chen, X., Wang, H., Wu, H., Jin, X., and Huang, C. (2017). Improved performances of lithium-ion batteries with a separator based on inorganic fibers. *J. Mater. Chem. A* 5, 311–318. doi: 10.1039/C6TA08404D
- Wu, D., Shi, C., Huang, S., Qiu, X., Wang, H., Zhan, Z., et al. (2015). Electrospun nanofibers for sandwiched polyimide/poly(vinylidene fluoride)/polyimide separators with the thermal shutdown function. *Electrochim. Acta* 176, 727–734. doi: 10.1016/j.electacta.2015.07.072
- Xiao, Q., Li, Z., Gao, D., and Zhang, H. (2009). A novel sandwiched membrane as polymer electrolyte for application in lithium-ion battery. *J. Membrane Sci.* 326, 260–264. doi: 10.1016/j.memsci.2008.10.019
- Xiao, W., Li, X., Guo, H., Wang, Z., Zhang, Y., and Zhang, X. (2012). Preparation of core-shell structural single ionic conductor SiO<sub>2</sub>@Li<sup>+</sup> and its application in PVDF-HFP-based composite polymer electrolyte. *Electrochim. Acta* 85, 612–621. doi: 10.1016/j.electacta.2012.08.120
- Xiao, W., Zhao, L., Gong, Y., Liu, J., and Yan, C. (2015). Preparation and performance of poly(vinyl alcohol) porous separator for lithium-ion batteries. *J. Membrane Sci.* 487, 221–228. doi: 10.1016/j.memsci.2015.04.004
- Xie, H., Liao, Y., Sun, P., Chen, T., Rao, M., and Li, W. (2014). Investigation on polyethylene-supported and nano-SiO<sub>2</sub> doped poly(methyl methacrylate-co-butyl acrylate) based gel polymer electrolyte for high voltage lithium ion battery. *Electrochim. Acta* 127, 327–333. doi: 10.1016/j.electacta.2014.02.038
- Xu, S., Cheng, Y., Zhang, L., Zhang, K., Huo, F., Zhang, X., et al. (2018). An effective polysulfides bridgebuilder to enable long-life lithium-sulfur flow batteries. *Nano Energy* 51, 113–121. doi: 10.1016/j.nanoen.2018.06.044
- Yang, P., Liu, L., Li, L., Hou, J., Xu, Y., Ren, X., et al. (2014). Gel polymer electrolyte based on polyvinylidene fluoride-co-hexafluoropropylene and ionic liquid for lithium ion battery. *Electrochim. Acta* 115, 454–460. doi: 10.1016/j.electacta.2013.10.202
- Zhang, F., Ma, X., Cao, C., Li, J., and Zhu, Y. (2014). Poly(vinylidene fluoride)/SiO<sub>2</sub> composite membranes prepared by electrospinning and their excellent properties for nonwoven separators for lithium-ion batteries. *J. Power Sources* 251, 423–431. doi: 10.1016/j.jpowsour.2013.11.079
- Zhang, J., Chen, S., Xie, X., Kretschmer, K., Huang, X., Sun, B., et al. (2014). Porous poly(vinylidene fluoride-co-hexafluoropropylene) polymer membrane with sandwich-like architecture for highly safe lithium ion batteries. *J. Membrane Sci.* 472, 133–140. doi: 10.1016/j.memsci.2014.08.049
- Zhao, H., Deng, N., Ju, J., Li, Z., Kang, W., and Cheng, B. (2019). Novel configuration of heat-resistant gel polymer electrolyte with electrospun poly(vinylidene fluoride-co-hexafluoropropylene) and poly-m-phenyleneisophthalamide composite separator for high-safety lithium-ion battery. *Mater. Lett.* 236, 101–105. doi: 10.1016/j.matlet.2018.10.067
- Zheng, H., Xie, Y., Xiang, H., Shi, P., Liang, X., and Xu, W. (2018). A bifunctional electrolyte additive for separator wetting and dendrite suppression in lithium metal batteries. *Electrochim. Acta* 270, 62–69. doi: 10.1016/j.electacta.2018.03.089
- Zhou, R., Liu, W., Yao, X., Leong, Y. W., and Lu, X. (2015). Poly(vinylidene fluoride) nanofibrous mats with covalently attached SiO<sub>2</sub> nanoparticles

- as an ionic liquid host: enhanced ion transport for electrochromic devices and lithium-ion batteries. *J. Mater. Chem. A* 3, 16040–16049. doi: 10.1039/C5TA02154E
- Zhou, X., Yue, L., Zhang, J., Kong, Q., Liu, Z., Yao, J., et al. (2013). A core-shell structured polysulfonamide-based composite nonwoven towards high power lithium ion battery separator. *J. Electrochem. Soc.* 160, A1341–A1347. doi: 10.1149/2.003309jes
- Zhu, Y., Wang, F., Liu, L., Xiao, S., Chang, Z., and Wu, Y. (2013). Composite of a nonwoven fabric with poly(vinylidene fluoride) as a gel membrane of high safety for lithium ion battery. *Energy Environ. Sci.* 6, 618–624. doi: 10.1039/C2EE23564A
- Zuo, P., Hua, J., He, M., Zhang, H., Qian, Z., Ma, Y., et al. (2017). Facilitating the redox reaction of polysulfides by an electrocatalytic layer-modified separator for lithium–sulfur batteries. *J. Mater. Chem. A* 5, 10936–10945. doi: 10.1039/C7TA02245J

**Conflict of Interest Statement:** The authors declare that the research was conducted in the absence of any commercial or financial relationships that could be construed as a potential conflict of interest.

Copyright © 2019 Liu, Ren, Zhang and Zhang. This is an open-access article distributed under the terms of the Creative Commons Attribution License (CC BY). The use, distribution or reproduction in other forums is permitted, provided the original author(s) and the copyright owner(s) are credited and that the original publication in this journal is cited, in accordance with accepted academic practice. No use, distribution or reproduction is permitted which does not comply with these terms.